

PACS numbers: 42.55.Px; 42.60.Lh
DOI: 10.1070/QE2013v043n10ABEH015139

Effect of thermal processes on critical operation conditions of high-power laser diodes

V.V. Parashchuk, Vu Doan Mien

Abstract. **Using numerical and analytical techniques in a three-dimensional approximation, we have modelled the effect of spatial thermoelastic stress nonuniformity in a laser diode–heat sink system on the output characteristics of the device in different operation modes. We have studied the influence of the pulse duration, the geometry of the laser system and its thermophysical parameters on the critical pump current density, in particular for state-of-the-art heat conductive substrate materials. The proposed approach has been used to optimise the laser diode assembly process in terms of the quality of laser crystal positioning (bonding) on a heat sink.**

Keywords: *high-power laser diodes, laser diode–heat sink (contact layer) system, nonuniform thermal fields, thermoelastic stresses, critical operation conditions, diamond heat sinks, chip positioning.*

1. Introduction

One well-known characteristic feature of semiconductor laser diodes (LDs) is that their lasing threshold is a (weak or strong) function of temperature [1, 2]. For this reason, thermal processes in LDs are receiving a great deal of attention. As shown as early as the 1960s, a diode experiences considerable thermoelastic stresses (TS's) during fabrication and operation, which are capable of causing microfractures and irreversible degradation of energy parameters in the case of injection lasers. In connection with this, an important issue is the ability to optimise the operation conditions of LDs through comparison of the critical conditions caused by TS generation with the extreme conditions determined by the temperature dependence of the threshold current density. This issue was addressed in detail by Kruzhilin et al. [3] for a one-dimensional system with application to the thermoelastic stress arising from spatial nonuniformity of the thermal field in the medium (one of the most important cases of TS's). A number of studies examined the role of other types of thermoelastic stress, in particular that generated when a heterostructure is secured (soldered) to a cooling line [4] and under other conditions (see e.g. Ref. [5]). However, since the thermoelasticity problem in the case of a nonuniform spatial temperature distribution in the active region is essentially three-dimensional [6–10], further work in this direction appears important. In this paper, using a method developed for evaluating the thermal field and TS in a system, we consider the problem of optimal laser chip positioning (bonding or connection) on heat sinks under various conditions. We present comparative computation results for efficient heat sink materials, as a continuation of our previous studies aimed at improving the efficiency of high-power diode structures with the use of diamond heat sinks [11].

V.V. Parashchuk B.I. Stepanov Institute of Physics, National Academy of Sciences of Belarus, prosp. Nezavisimosti 68, 220072 Minsk, Belarus; e-mail: v.parashchuk@ifanbel.bas-net.by;
Vu Doan Mien Institute of Materials Science, Vietnamese Academy of Science and Technology (VAST), 18 Hoang Quocs Viet. Str., Cau Giay District, Hanoi, Vietnam

Received 31 January 2013; revision received 12 March 2013
Kvantovaya Elektronika **43** (10) 907–913 (2013)
Translated by O.M. Tsarev

2. Modelling of the spatial distribution of thermal fields in the laser system under investigation

To analyse the thermoelastic stress in a diode–heat sink system approaching a real laser system, consider a spatial distribution of thermal fields that takes into account thermophysical processes in the contact layers using the three-dimensional steady-state heat equation (1) with appropriate boundary conditions given by (2)–(5) (Fig. 1):

$$\frac{\partial^2 T}{\partial x^2}+\frac{\partial^2 T}{\partial y^2}+\frac{\partial^2 T}{\partial z^2}=0, \tag{1}$$

$$\lambda_1 \frac{\partial T_1}{\partial Z}\Big|_{Z=z} =$$

$$\begin{cases} -q & \text{for } \varepsilon-0.5l_1 \leqslant x \leqslant \varepsilon+0.5l_1, \eta-0.5l_2 \leqslant y \leqslant \eta+0.5l_2, \\ 0 & \text{at the other points on the upper crystal facet,} \end{cases} \tag{2}$$

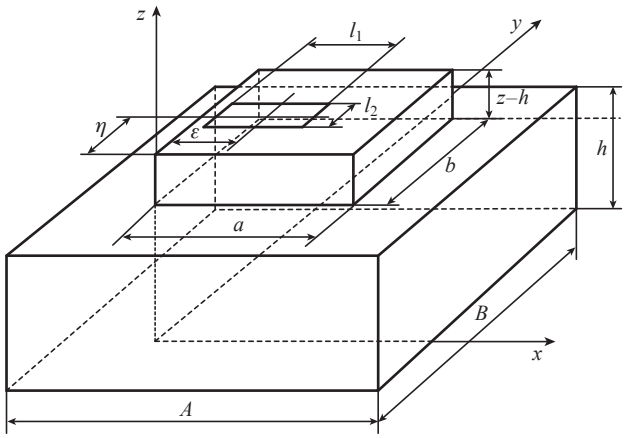

Figure 1. Mathematical model of system (1)–(5).

$$T_1|_{z=h} = T_2|_{z=h} \ (x,y) \in (a,b), \ T_2|_{z=0} = T_0, \tag{3}$$

$$\lambda_1 \frac{\partial T_1}{\partial z}\Big|_{z=h} = \lambda_2 \frac{\partial T_2}{\partial z}\Big|_{z=h}, \ (x,y) \in (a,b),$$

$$\frac{\partial T_2}{\partial z}\Big|_{z=h} = 0, \ (x,y) \notin (a,b), \tag{4}$$

$$\frac{\partial T_1}{\partial x}\Big|_{\substack{x=0,\\x=a}} = \frac{\partial T_1}{\partial y}\Big|_{\substack{y=0,\\y=b}} = \frac{\partial T_2}{\partial x}\Big|_{\substack{x=(a-A)/2,\\x=(a+A)/2}}$$

$$= \frac{\partial T_2}{\partial y}\Big|_{\substack{y=(b-B)/2,\\y=(b+B)/2}} = 0, \tag{5}$$

where $T_1(x, y, z)$ and $T_2(x, y, z)$ are the temperatures in the bulk of the crystal and heat sink (substrate or contact layer), respectively; $\lambda_{1,2}$ are their thermal conductivities; a, b, $z-h$, A, B and h are the dimensions of the crystal and heat sink; $l_{1,2}$ are the dimensions of the heat source (e.g., of the active region); ε and η are the coordinates of the centre of the source; q is its power per unit surface area; and T_0 is the (constant or variable) temperature of the lower heat sink surface. In this model, the source has the form of a rectangle situated on the crystal surface, which corresponds in some measure to the structure of a real LD with an asymmetric position of the active region near one of the boundary surfaces. Given the small thickness of this region (~1 μm), the heat distribution in it is taken to be two-dimensional (in the xy plane).

Analytically solving Eqn (1) subject to the boundary conditions (2)–(5) through separation of variables, we obtain

$$T(x,y,z) = T_0 + ql_1l_2\left(\frac{h}{AB\lambda_2} + \frac{z-h}{ab\lambda_1}\right) + \frac{4qal_2}{\lambda_1 b\pi^2}$$

$$\times \sum_{k=1}^{\infty} \frac{1}{k^2} \cos\left(\frac{k\pi}{a}x\right)\cos\left(\frac{k\pi}{a}\varepsilon\right)\sin\left(\frac{k\pi}{2a}l_1\right)\left[\tanh\left(\frac{k\pi}{a}(z-h)\right)\right.$$

$$\left. + \frac{[\lambda_1 A/(\lambda_2 a)]\tanh(k\pi h/A)}{1 + [\lambda_1 A/(\lambda_2 a)]\tanh(k\pi h/A)\tanh(k\pi(z-h)/a)}\right] + \frac{4qbl_1}{\lambda_1 a\pi^2}$$

$$\times \sum_{m=1}^{\infty} \frac{1}{m^2} \cos\left(\frac{m\pi}{b}y\right)\cos\left(\frac{m\pi}{b}\eta\right)\sin\left(\frac{m\pi}{2b}l_2\right)\left[\tanh\left(\frac{m\pi}{b}(z-h)\right)\right.$$

$$\left. + \frac{[\lambda_1 B/(\lambda_2 b)]\tanh(m\pi h/B)}{1 + [\lambda_1 B/(\lambda_2 b)]\tanh(m\pi h/B)\tanh(m\pi(z-h)/b)}\right] + \frac{16q}{\lambda_1\pi^3} \tag{6}$$

$$\times \sum_{k=1}^{\infty}\sum_{m=1}^{\infty} \frac{1}{km\sqrt{k^2/a^2 + m^2/b^2}} \cos\left(\frac{m\pi}{b}y\right)\cos\left(\frac{k\pi}{a}x\right)$$

$$\times \sin\left(\frac{m\pi}{2b}l_2\right)\sin\left(\frac{k\pi}{2a}l_1\right)\cos\left(\frac{m\pi}{b}\eta\right)\cos\left(\frac{k\pi}{a}\varepsilon\right)$$

$$\times \left\{\tanh[(z-h)\sqrt{k^2\pi^2/a^2 + m^2\pi^2/b^2}] + \frac{\lambda_1\sqrt{k^2/a^2 + m^2/b^2}}{\lambda_2\sqrt{k^2/A^2 + m^2/B^2}}\right.$$

$$\times \tanh(h\sqrt{k^2\pi^2/A^2 + m^2\pi^2/B^2})\Big\}\Big\{1 + \frac{\lambda_1\sqrt{k^2/a^2 + m^2/b^2}}{\lambda_2\sqrt{k^2/A^2 + m^2/B^2}}$$

$$\times \tanh(h\sqrt{k^2\pi^2/A^2 + m^2\pi^2/B^2})$$

$$\left. \times \tanh[(z-h)\sqrt{k^2\pi^2/a^2 + m^2\pi^2/b^2}]\right\}^{-1}.$$

The thermal fields computed in the above model are presented (as sections) in Fig. 2. The following thermal conductivity values were taken: $\lambda_1 = 400$ W m^{-1} K^{-1} for a copper heat sink (Fig. 2a) and 1450 W m^{-1} K^{-1} for a diamond heat sink (Figs 2b, 2c) and $\lambda_2 = 50$ W m^{-1} K^{-1} for the GaAs crystal. Using the above solution to (6), we have demonstrated the possibility of taking into account additive interaction between several (two) heat sources, e.g. elements of a laser diode structure. For simplicity, the two sources were taken to have identical dimensions (0.45×0.1 mm) and differ in power ($P_{1,2}$). The crystal and heat sink had identical dimensions. The centre-to-centre distance between the elements was $\delta_x = 0.5$ mm.

We optimised computation conditions in a Matematika environment: a predetermined accuracy in temperature distribution computation (0.0001–0.001) was ensured at each point (x, y) at minimum summation indices $(k, m) \sim 20–40$.

3. Computation of the spatial distribution of thermoelastic stresses in the laser system

General formulation of the problem of finding the thermoelastic stress from a given heat flux distribution is well known [6–8], and the problem can be solved in particular cases.

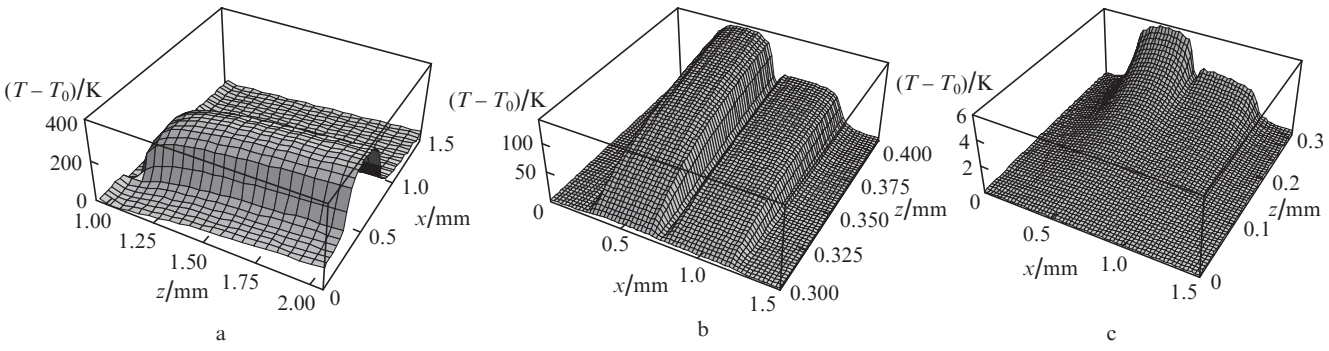

Figure 2. Thermal field distribution in the model system: (a, b) crystal and (c) heat sink with (a) one and (b, c) two heat sources. Parameters of the system: $l_1 = 0.45$ mm, $l_2 = 0.1$ mm, $a = b = A = B = 1.5$ mm, $h = 0.3$ mm, $\delta_x = 0.5$ mm, $\varepsilon = 0.5$ mm, $\eta = y = 0.75$ mm, (a) $P = 10$ W, (b) $P_1 = 4.5$ W, $P_2 = 2.25$ W.

Consider an approximation in which the region under consideration can be broken down into small elements. Within each element, a quasi-three-dimensional thermoelasticity problem can then be formulated. It can be shown based on existing ideas [6] that the solution to a standard system of equations of balance subject to appropriate boundary conditions and strain compatibility constraints for stress determination has then the form

$$\sigma_{ij} = \beta_{ij}\left[\frac{3(z-d/2)}{2(d/2)^3}\,\overline{zT(x,y,z)} + \overline{T(x,y,z)} - T(x,y,z)\right]$$

$$(i,j=1,2), \qquad \Delta = \begin{vmatrix} s_{11} & s_{12} & s_{16} \\ s_{12} & s_{22} & s_{26} \\ s_{16} & s_{26} & s_{66} \end{vmatrix}, \qquad (7)$$

where $\beta_{ij} \equiv \beta_m = A_{mn}\alpha_n/\Delta$ are the thermoelastic coefficients (m, n = 1, 2, 6); A_{mn} is the algebraic complement of s_{mn} (elastic constants) in the determinant Δ; α_n is the thermal expansion coefficient; and the overbar in (7) means averaging over a layer of thickness d. In an isotropic medium, $\beta_{ij} = \alpha_T E/(1-\nu)$, where α_T is the linear thermal expansion coefficient; ν is Poisson's ratio; and E is Young's modulus.

The thermoelastic stress ($\sigma \equiv D$) in the model system was computed as a function of heat source power (P), thermal conductivity of the substrate material (copper and diamond) and geometry of the elements of the system (Fig. 3).

It follows from the computation results that, at a heat source power $P \sim 1$ W, the thermoelastic stress varies across the structure (along the z axis) in the range $\pm(1-10)$ MPa, which is comparable to the residual stress arising from the thermal expansion mismatch between neighbouring layers in a multilayer structure. The highest temperature (overheating) in this region is $\Delta T = 35-40$ K. At $P = 10$ W (power density of $\sim 10^6$ W cm^{-2}), we have $\sigma \approx \pm(10-200)$ MPa (Fig. 3a) and $T_{max} \sim 400-450$ K (Fig. 2a), i.e. the thermoelastic stress prevails and the active-region overheating is significant ($\Delta T \sim$ 100 K), in agreement with previous data [3, 12–15]. Calculation in the one-dimensional approximation [5] leads to underestimation of both σ and T_{max} by one to two orders of magnitude. Because of this, under the above conditions the contribution of the stress in question (relative to the residual stress) cannot be neglected in thermoelasticity problems.

Comparison of computation results for different heat sinks indicates that, in the case of a copper heat sink, the thermoelastic stress within the active region is somewhat lower than that in the case of a diamond heat sink even though the thermal expansion coefficients of these heat sink materials differ significantly from that of the active medium (the difference is greater in the case of diamond). At the same time, the T_{max} of copper heat sinks is markedly higher (by a factor of 1.5). Beyond the active region, the opposite relationship between the stresses holds. Since the magnitude and sign of the thermoelastic stress depend on spatial localisation in the system and the thermophysical properties of the heat sink material, this circumstance can be used to make the stress constant throughout the length of the active region. The effectiveness (degree) of such equalisation is markedly higher in the case of diamond heat sinks. Figure 3b shows the spatial distribution of thermoelastic stresses in the model system with 'thermal interaction' (in the additivity approximation) between several sources, exemplified by two elements.

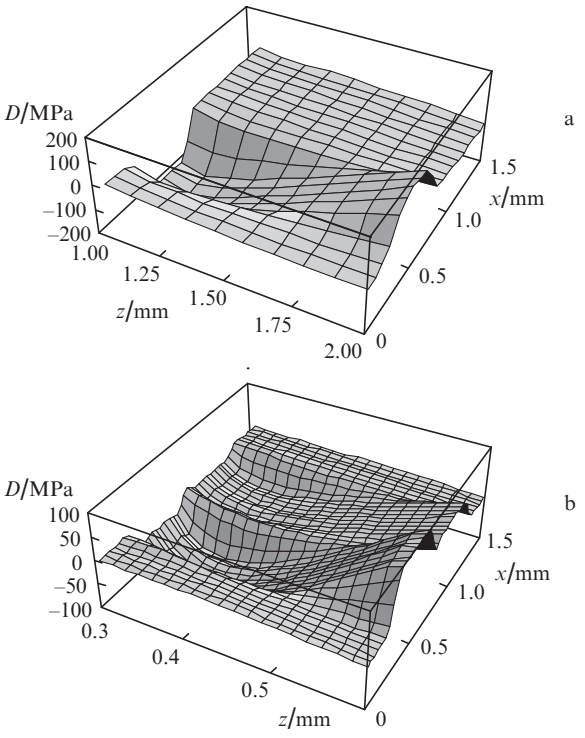

Figure 3. Spatial distribution of thermoelastic stresses for (a) one (P = 10 W) and (b) two heat sources ($\varepsilon_1 = 0.5$ mm, $\varepsilon_2 = 1$ mm, $P_1 = 10$ W, $P_2 =$ 5 W). Parameters of the system: $l_1 = 0.45$ mm, $l_2 = 0.1$ mm, $a = b =$ 1.5 mm, $A = B = 5$ mm, $h = 0.3$ mm, $\eta = b/2$, $\varepsilon = 0.5$ mm, $y = b/2$.

4. Effect of thermoelastic stress on the output characteristics of a laser in different operation modes

Following Kruzhilin et al. [3], we will attempt to optimise the operation conditions of a laser diode by comparing the critical conditions caused by TS generation to the extreme conditions determined by the temperature dependence of the threshold current density in a given approximation.

Consider first an unsteady-state (pulsed) mode. It is known that the problem of thermoelasticity in pulsed mode can be solved in a quasi-static approach at pulse durations of up to several nanoseconds, even though the heat conduction problems in pulsed and continuous modes differ significantly. Using previous results [9], the solution to the corresponding heat equation can be written in the form

$$T(x,y,z,t) = \frac{1}{(2\varkappa\sqrt{\pi t})^3}\int_0^a\int_0^b\int_0^{c-h}\varphi(\xi,\eta,\zeta)$$

$$\times\exp\left[-\frac{(\xi-x)^2+(\eta-y)^2+(\zeta-z)^2}{4\varkappa t}\right]d\xi d\eta d\zeta, \qquad (8)$$

where t is time; T is the absolute temperature; a, b and $c-h$ are the dimensions of the active region; $\varphi(\xi, \eta, \zeta) = T(x, y, z, 0)$ is the initial temperature distribution, which can be represented by (6); $\varkappa = \lambda/(c_{sp}\rho)$ is the thermal diffusivity of the crystal; c_{sp} is its specific heat; ρ is its density; and λ is its thermal conductivity.

First, the temperature field $\Delta T = T(x, y, z, t) - T(x, y, z, 0)$ was computed in a simplified laser model (with no massive heat sink). The corresponding spatial distribution of thermo-

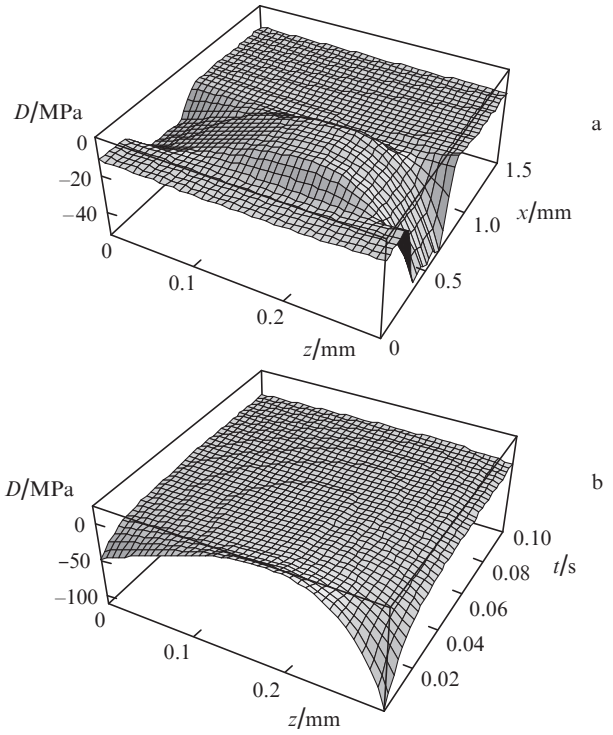

Figure 4. (a) Thermoelastic stress in the model system under time-dependent excitation in the *XZ* section; (b) Time-dependent TS. Parameters of the system: $P = 10$ W, $a = b = 1.5$ mm, $z = c = 0.3$ mm, $T_0 = 0$, $\lambda = 0.5$ W cm^{-1} K^{-1}, Z = 0.27 cm^2 s^{-1}, $l_1 = 0.45$ mm, $l_2 = 0.1$ mm, $\varepsilon = 0.5$ mm, $\eta = 0.75$ mm, $t = 0.01$ s (a), $y = b/2$, $x =$ (b).

elastic stresses in the approximation defined by (6)–(8) is presented in Fig. 4.

The spatial distributions of thermal fields and thermoelastic stresses can be related to performance parameters of the laser diode through the dependence of the heat flux q on the pump current density j in the laser diode and the temperature dependence of the threshold current density in the form

$$q = Vj, \quad j_{th} = j_{0th}\exp(\Delta T/T_1), \tag{9}$$

where V is the voltage across the p–n junction and j_{0th} is the threshold current density at the initial temperature of the medium, T_0. The value of q determines the boundary conditions (2) and the spatial temperature distribution (6). From (8) and (9), we obtain a relation for the critical current density or a dimensionless lasing condition in terms of thermoelastic stress, analogous to previous results [3]:

$$j' = F_1(t')^{-3/2}. \tag{10}$$

Here, $j' = j/j_{0th}$ is the dimensionless critical current density (at which irreversible structural changes in the diode are possible); $t' = t/t_1 \equiv t_p$ is the dimensionless pump current pulse duration; $F_1 \sim \sigma_{ij}/(\beta_{ij}T_1)$ is a dimensionless parameter (a function of coordinates); $\sigma_{ij} = \sigma_{cr}$ is the allowable thermoelastic stress in the active medium; $T_1 \sim 80$ K is the characteristic temperature; and $t_1 = \pi\lambda c_{sp}\rho T_1^2/(j_{0th}V)^2$.

The lasing condition in terms of threshold current density has the same form as in Kruzhilin et al. [3],

$$j' \geqslant \exp(j'\sqrt{t'}), \tag{11}$$

and determines the current density at which lasing terminates at time t'. Equation (11) has two real solutions for $t' < e^{-2}$ and determines the limiting laser pulse duration $t_{lim} = \pi\lambda c_{sp}\rho T_1^2/(ej_{0th}V)^2$ (for $t' \geqslant e^{-2}$).

The optimal diode operation mode can be established by comparing criteria (10) and (11). As an example, Fig. 5 presents a numerical solution to Eqn (10) [curves (*1*)–(*3*)] for different conditions and a solution to Eqn (11) [curve (*4*)]. It is seen that, for $t' > e^{-2}$, pulsed lasing is impossible. For $t' < e^{-2}$, the equality in (11) is met at two current densities (the lower and upper branches of the plot), corresponding to the onset of lasing (first threshold) and quenching of lasing due to overheating of the p–n junction (second threshold). The largest divergence between the branches determines the current density at which the highest output power is reached (at a constant pulse duration). The curves intermediate between the two branches, determined by the TS mechanism, represent optimal lasing conditions. It is worth noting that the $j'(t')$ dependence obtained from (10) is multivalued and is a function of coordinates (we present the dependence for three X values, with the other parameters fixed) as a consequence of the nonuniformity of the spatial distributions of the thermal field and thermoelastic stresses (Fig. 4).

It follows from the data obtained that, at varied values of the parameter F_1 (coordinates), heat source power P and other parameters and a constant laser pulse duration, the current density can be limited by both the quenching of lasing because of the increase in threshold current density with temperature and the development of the critical thermoelastic stress. In particular, at the optimal pulse duration $t' = 0.04$ [3], which allows the maximum output energy to be obtained, it can be deduced from Fig. 5b that, at $x = 0.275$ mm [curve (*3*)], the output power is determined by the current limitation due to TS development, whereas at $x = 0.3$ and 0.5 mm it is determined by the temperature dependence of the threshold current density.

With increasing excitation pulse duration (i.e. as a steady state is approached), the effect of the nonuniformity of the spatial distribution of the thermal field increases, in agreement with data in the literature. It is then necessary to take into account the three-dimensional temperature field distribution in order to evaluate the TS contribution to the spatial $j_{cr} \equiv j'$ distribution. On the whole, in pulsed mode the effect of TS on critical characteristics prevails over the limitation due to the temperature dependence of the threshold current.

Similar results were obtained for a laser system with a massive heat sink and different heat sink materials (copper, diamond and cubic boron nitride). It has been shown that the use of highly efficient diamond heat sinks allows the critical pump current density to be increased by almost a factor of 2 (relative to copper heat sinks) and considerably extends the functional capabilities of the device in terms of its energetic and dynamic parameters.

In a steady state (continuous mode), the conditions for lasing in terms of thermoelastic stress and threshold current density have the form

$$j' = F_2(F)^{-1}, \tag{12}$$

$$j' \geqslant \exp(j'F), \tag{13}$$

where the parameter F_2 is an analogue of F_1 and, in contrast to previous results [3], is a function of coordinates; $F = j_{0th}Vz \times (2\lambda_2 T_1)^{-1}$ is a dimensionless variable; and λ_2 is the thermal

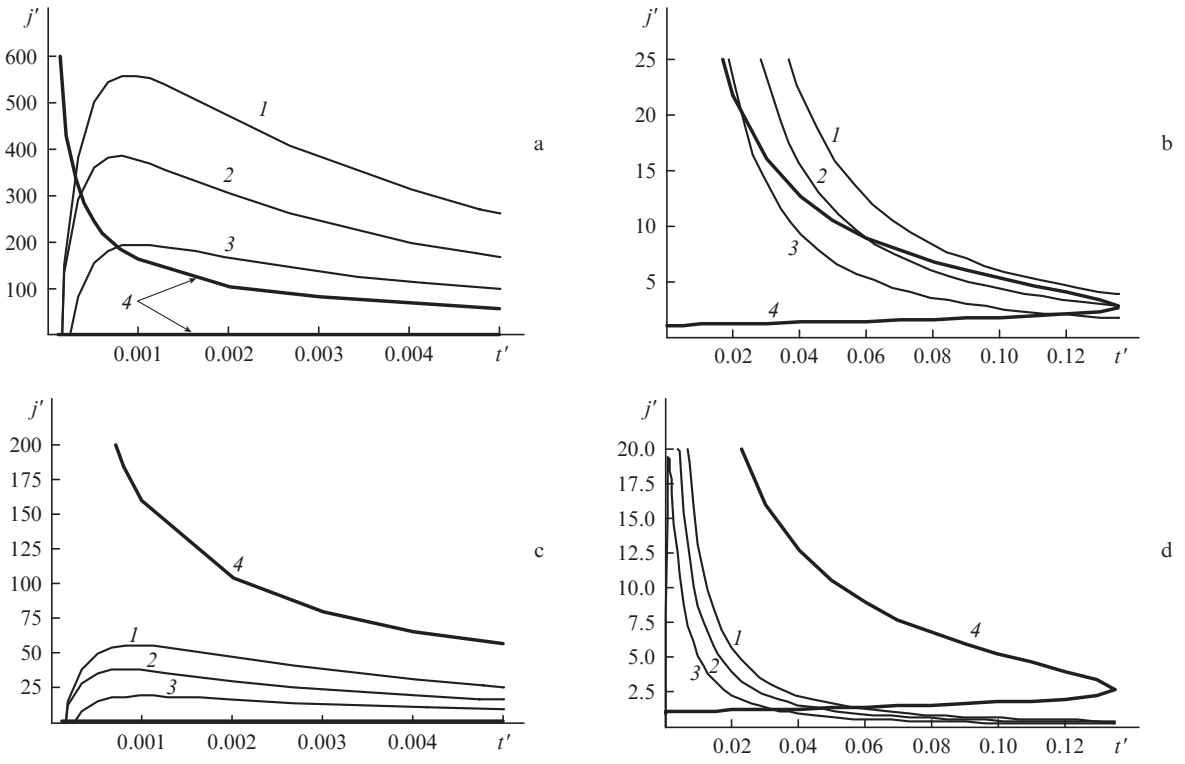

Figure 5. Time dependences of the critical current through a laser system with a copper heat sink at a heat source power P = (a, b) 10 and (c, d) 1 W. Parameters of the system: $a = b = 1.5$ mm, $z = c = 0.3$ mm, $T_0 = 0$, $\lambda = 0.5$ W cm^{-1} K^{-1}, 0.27 cm^2 s^{-1}, $l_1 = 0.45$ mm, $l_2 = 0.1$ mm, $\varepsilon = 0.5$ mm, $\eta = 0.75$ mm, $y = b/2$, x = (*1*) 0.5, (*2*) 0.3 and (*3*) 0.275 mm. Curve (*4*) represents a solution to Eqn (11).

conductivity of the heat sink material. The solutions meeting criteria (12) and (13) are qualitatively similar to the above case of an unsteady state.

It follows from the simulation results that, in a steady state, nonuniformity of the spatial temperature distribution has a weak effect on the $j'(F)$ dependence compared to pulsed mode. Lasing characteristics in the region of the active layer are limited predominantly by the temperature dependence of the threshold current, which correlates with the described effect of pulse duration on the unsteady-state behaviour of the system.

To experimentally verify the described effect of thermal processes in different LD operation modes, we can use recommendations by Kruzhilin et al. [3], namely, the characteristic dependence of the critical current density on various parameters. In particular, it follows from criterion (10) that, at sufficiently short pulse durations, the current density j_{cr} should be proportional to $t_p^{-3/2}$ rather than to $t_p^{-1/2}$ [3]. Moreover, the parameters F_1 and F_2 in (10) and (12) should be spatially nonuniform.

5. Optimisation of chip positioning methods and the assembly process

It is known that laser chip mounting (positioning) on heat sinks in the LD assembly process has a significant effect on many characteristics of the LDs, with the strongest influence on thermal conditions and, as a consequence, on the energetic parameters and lifetime of the devices [16]. The corresponding requirement can be formulated in terms of the displacement $\Delta\varepsilon$ of the output (front) mirror of the chip relative to the working edge of the heat sink. The permissible displacement (to avoid radiation vignetting) should be several microns. Below, in the approach considered above we numerically simulate the effect of laser chip positioning on the spatial TS distribution in a laser system (Fig. 6) and optimise the conditions of the process.

We use the $\sigma_{ij} = \sigma_{ij}(x, y)$ $(i, j = 1, 2, 3)$ approximation [10] under various conditions, in particular, without (limiting conditions) and with a heat sink, and present results for the normal stress tensor component $\sigma_{xx} \equiv D$, which has the highest value (a part of the crystal is shown). To simplify computation, we used interpolation with quadratic or higher degree polynomials. The parameters of the problem were evaluated by analysing the generalised Hooke's law and Saint-Venant's strain balance and compatibility conditions using appropriate boundary conditions and an Airy stress function [7, 10].

When the active region (source) stripe is located in the centre of the crystal, the TS pattern is symmetrical with respect to the section parallel to the *xoz* plane and passing through the longitudinal axis of the stripe and with respect to arbitrary cross sections parallel to the *yoz* plane, i.e. for the opposite sides of the active region. It can be seen that stress concentrates predominantly at the perimeter of the source (in its peripheral parts). The stresses on the long and short sides of the stripe may have the same sign or differ in sign. Moreover, the sign of the stress may change on a given side of the stripe. These results correlate to some extent with residual stress data obtained previously [4] by the finite element method for a diode bonded on a heat sink (contact problem).

Displacement of the source to the edge of the crystal distorts the symmetry of the above stress pattern. When the short side (front edge) of the source coincides with the working face *yoz* of the crystal, σ_x has the lowest value or

approaches zero, which corresponds to precise positioning, $\Delta\varepsilon = 0$ (Fig. 6a). Such a situation occurs both with and without a heat sink. A deviation from the above conditions with the outer projection (or inner ledge) of the front edge, $\Delta\varepsilon$, exceeding ± 5 μm leads to a stress spike in the corresponding region, which considerably exceeds (by several times) the maximum stress on the other sides of the source. This fact can be used to assess the laser chip mounting quality and as an effective positioning method in the diode structure assembly process. It also follows from our simulation results that the use of a heat sink leads to a considerable relative reduction in the thermoelastic stress spike at the front edge of the active region at reduced positioning accuracy.

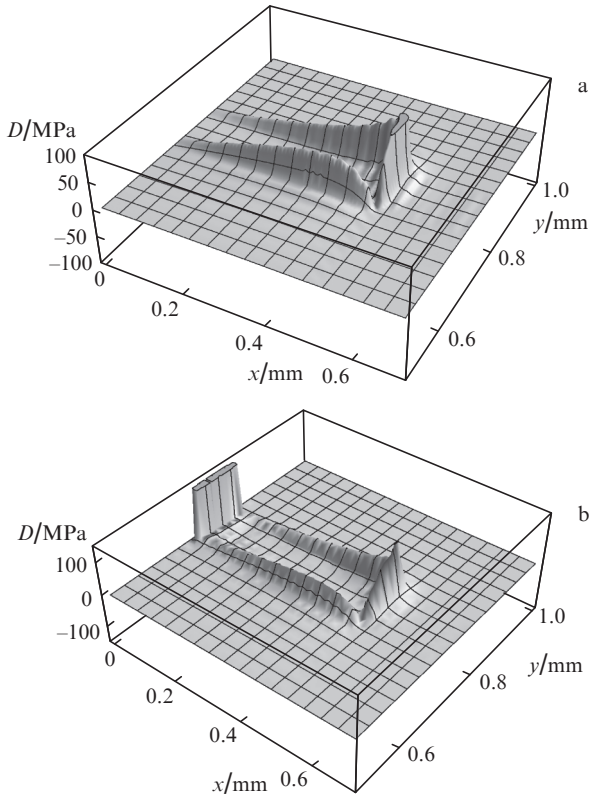

Figure 6. Effect of the displacement of the laser chip, $\Delta\varepsilon$, on the magnitude and distribution of the thermoelastic stress in the model system: $\Delta\varepsilon$ = (a) 0 and (b) ± 5 μm. Parameters of the system: $P = 1$ W, $\lambda = 0.05$ W mm^{-1} K^{-1}, $a = b = 1.5$ mm, $c = 0.3$ mm, $l_1 = 0.5$ mm, $l_2 = 0.1$ mm.

Using the approach in question, which takes into account the thermoelastic stress, we analysed the influence of the longitudinal and transverse positioning geometries on the active-region overheating (ΔT) for copper and diamond heat sinks. The results indicate that, in the case of longitudinal positioning (along the x axis), ΔT depends significantly on a number of factors: the geometry of the crystal (heat sink) and active region, heat source power P, thermophysical characteristics of the materials used and the temperature of the ambient medium, T_0. In most of the configurations considered, both pulsed and continuous modes are possible at $\Delta\varepsilon \sim 1-5$ μm. In the case of longitudinal positioning, only pulsed mode with the use of a diamond heat sink is possible.

It is shown that the active-region overheating depends as well on the accuracy of transverse chip positioning, along the y axis, i.e. on the degree of chip 'decentring' in the mounting process. It is, therefore, important to take into account this factor, along with longitudinal positioning in device assembly. Simulation results indicate that there is an optimal degree of decentring for minimising the overheating. Like in the case of longitudinal positioning, simulation predicts that, at high ΔT values, only pulsed mode with the use of efficient heat sinks is possible at a power $P \sim 10$ W ($T_0 \sim 300$ K). In other cases, both pulsed and continuous modes are possible under the above conditions. The above results make it possible to optimise the entire process of assembling laser diodes and diode-based optical modules.

6. Conclusions

Using numerical and analytical techniques and considering a laser system approaching a real one, we have modelled the effect of the thermoelastic stress arising from a spatial nonuniformity of the thermal field on the output characteristics of an injection laser in different operation modes. The results indicate that, in the case of high-power LDs (at heat fluxes above 10^6 W cm^{-2}), this stress is comparable in magnitude to the residual internal stress due to the multilayer nature of the heterostructures, and that under such conditions there is appreciable active-region overheating ($\Delta T \geqslant 100$ K). The use of diamond heat sinks improves the spatial uniformity of the thermoelastic stress in the laser system.

We have performed a comparative analysis of critical operation conditions associated with the TS and the temperature dependence of the threshold pump current density. Nonuniformity of the spatial distribution of the thermal field is shown to have a significant effect on the current and the critical current limitation mechanism. In pulsed mode, the effect of TS on critical characteristics prevails over the limitation due to the temperature dependence of the threshold current. We have studied the influence of the pulse duration, the geometry of the laser system and its thermophysical parameters on the critical pump current density, in particular for a diamond heat sink, and optimised diode operation under such conditions.

Using a method developed for evaluating thermal fields and thermoelastic stresses, we numerically modelled optimal conditions for laser crystal (chip) mounting (positioning) on a heat sink. The results suggest that, in optimising process conditions, one should take into account not only the permissible ledge (displacement) of the front mirror of the chip relative to the working edge of the substrate but also chip decentring with respect to its axis of symmetry. These results make it possible to facilitate the positioning process and simplify the entire process of assembling diode lasers, thereby considerably improving the output characteristics of the devices.

Acknowledgements. This work was supported by the Belarusian Republican Foundation for Fundamental Research (International Project No. F09VN-007).

References

1. Alferov Zh.I. *Sb. Nauchn. Tr. Voen. Inst. Kievsk. Nats. Univ.*, **21**, 6 (2009).
2. Gribkovskii V.P. *Poluprovodnikovye lazery* (Semiconductor Lasers) (Minsk: Universitetskoe Izd., 1988).

3. Kruzhilin Yu.I., Shveikin V.I., Antonov N.V., Koloskov Yu.I. *Izv. Vyssh. Uchebn. Zaved. SSSR, Ser. Radioelektron.*, **12** (7), 692 (1969).
4. Sherstnev V.A., Kuz'min A.N., Ryabtsev G.I. *Vestsi Akad. Navuk BSSR*, **4**, 75 (1987).
5. Polyakov M.E. *Izv. Akad. Nauk BSSR, Ser. Fiz.-Mat. Nauk*, **5**, 71 (1981).
6. Grechushnikov B.N., Brodovskii D. *Kristallografiya*, **1**, 597 (1956).
7. Kupradze V.D., Gegelia T.G., Basheleishvili M.O., Burchuladze T.V. *Three-Dimensional Problems of the Mathematical Theory of Elasticity and Thermoelasticity* (Amsterdam: North-Holland, 1979; Moscow: Nauka, 1976).
8. Podstrigach Ya.S., Kolyano Yu.M. *Neustanovivshiesya temperaturnye polya i napryazheniya v tonkikh plastinakh* (Unsteady Temperature Fields and Stresses in Thin Plates) (Kiev: Naukova Dumka, 1972); *Obobshchennaya termomekhanika* (Generalised Thermomechanics) (Kiev: Naukova Dumka, 1976).
9. Koshlyakov N.S., Gliner E.B., Smirnov M.M. *Uravneniya v chastnykh proizvodnykh matematichskoi fiziki* (Partial Differential Equations of Mathematical Physics) (Moscow: Vysshaya Shkola, 1970).
10. Timoshenko S.P., Goodier J.N. *Theory of Elasticity* (New York: McGraw-Hill, 1970; Moscow: Nauka, 1979).
11. Parashchuk V.V., Ryabtsev G.I., Belyaeva A.K., et al. *Kvantovaya Elektron.*, **40** (4), 301 (2010) [*Quantum Electron.*, **40** (4), 301 (2010)].
12. Garnov S.V., Mikhailov V.A., Serov R.V., et al. *Kvantovaya Elektron.*, **37** (10), 910 (2007) [*Quantum Electron.*, **37** (10), 910 (2007)].
13. Smirnov V.A., Shcherbakov I.A. *Kvantovaya Elektron.*, **38** (12), 1105 (2008) [*Quantum Electron.*, **38** (12), 1105 (2008)].
14. Nannichi Y., Matsui J., Ishida K. *Jpn. J. Appl. Phys.*., **14**, 1561 (1975).
15. Bezotosnyi V.V., Kumykov Kh.Kh. *Kvantovaya Elektron.*, **25** (3), 225 (1998) [*Quantum Electron.*, **28** (3), 217 (1998)].
16. Brauch U., Loosen P., Opower H. *Top. Appl. Phys.*, **78**, 289 (2000).